Reversible electric field manipulation of the Dzyaloshinskii-Moriya interactions in transition metal dimers

Byungryul Jang and G. M. Pastor
Institut für Theoretische Physik, Universität Kassel, Heinrich-Plett-Straße 40, 34132 Kassel, Germany

(Received 22 March 2024; revised 26 June 2024; accepted 17 July 2024; published 30 July 2024)

The anisotropic antisymmetric Dzyaloshinskii-Moriya (DM) interactions between local magnetic moments $\boldsymbol{\mu}_i$ and $\boldsymbol{\mu}_j$, which can be induced by an external electric field (EF) are investigated in the framework of density functional theory by considering all $3d$, $4d$, and $5d$ freestanding transition metal dimers. The possibilities of triggering and reversibly tuning chiral magnetic couplings by electric means are demonstrated. The dependence of the DM-coupling vector $\boldsymbol{D}_{ij}$ on the EF strength E is shown to be approximately linear for $|E| \leqslant 0.6$ V/Å, with only minor third-order corrections. The first- and third-order zero-field electric susceptibility of the DM couplings are determined and analyzed as a function of d-band filling. The correlations between them and the chirality of the spin-orbit energy are displayed. From a microscopic perspective, the EF-induced DM couplings are shown to stem from the permanent electric dipole moments $\boldsymbol{p}^0$ that are already present in the field-free dimers whenever their local magnetic moments are not collinear. The symmetry rules governing $\boldsymbol{p}^0$ and its chirality are discussed. Finally, the dependence of the EF-induced DM couplings on the degree of noncollinearity of the magnetic order is quantified by varying systematically the angle θ between the local moments. While the electronic calculations show that the changes in the effective $\boldsymbol{D}_{ij}$ can be quite important for arbitrary θ, one also observes that $\boldsymbol{D}_{ij}$ depends weakly on θ and is thus transferable within a limited range of noncollinear magnetic arrangements, provided that they are not too far from the lowest-energy configuration.

DOI: 10.1103/PhysRevB.110.014443

I. INTRODUCTION

Low-dimensional magnetic materials such as clusters, one-dimensional (1D) chains, and thin film remain one of the most active and stimulating fields in fundamental and applied condensed-matter research. On the one hand, their remarkable size-, structural-, and dimensional-dependent behaviors offer multiple possibilities of tuning and optimizing the magnetic characteristics of materials for specific technological purposes, for example, for the development of high-density storage media, medical applications, and spin-electronic devices. On the other, from a fundamental perspective, considerable efforts are being dedicated to understanding magnetoanisotropic phenomena, which reflect the subtle effects of spin-orbit interactions on quantum many-body systems. One of the most fundamental manifestations of magnetic anisotropy is the dependence of the electronic energy on the spin-magnetization direction, defining the low-temperature orientation of the average magnetization, as well as its stability at finite temperatures or under the action of external fields. Recent investigations have also revealed the importance of the anisotropy of the interactions between the local magnetic moments, which are not only responsible for the shape and stability of the magnetic order but are also crucial for the dynamical response of magnetic materials to currents, laser pulses, and external fields. Particularly interesting are the antisymmetric anisotropic couplings, known as Dzyaloshinskii-Moriya (DM) interactions since they result in remarkable noncollinear magnetic orders with distinct chiralities, for example, spin-density waves, skyrmions, and other localized magnetic textures [1–8]. Therefore, elucidating the microscopic origin and quantitative values of the anisotropic magnetic interactions is a matter of central importance.

In past years, significant progress has been made in controlling the magnetic properties of nanostructures by external sources such as spin-polarized currents, laser fields, and static electric fields (EFs). In particular, the use of EFs appears as a very promising method of steering the spin degrees of freedom since it is both reversible and energy efficient. Recent experiments have in fact shown that an external EF can modify the magnetoanisotropic behavior of a large variety of materials including metal-oxide semiconductors, thin films, nanomagnets, and small clusters [9–21]. For instance, an EF-induced magnetization reversal has been achieved by modifying the interface exchange bias in multiferroic laminates [19] and the magnetization directions of nanomagnets have been manipulated by means of the EF generated by the tip of a scanning tunneling microscope [20,21].

The experimental results are supported by theoretical studies of the effects of EFs on molecules, clusters, multilayers, and surface nanostructures [22–33]. For example, Oba *et al.* have calculated the EF-induced modifications of the frozen-magnon dispersion relations and effective Heisenberg exchange couplings in a freestanding Fe monolayer and in a Co monolayer on Pt(111) within density functional theory (DFT) [30]. Moreover, the resulting changes in the Curie temperature of the films have been estimated by performing Monte Carlo simulations. Goerzen *et al.* have investigated the EF-assisted nucleation and annihilation of magnetic skyrmions in Pd/Fe/Ir(111) using a classical spin

model in which the interaction parameters are derived from DFT calculations [31]. Concerning the magnetoanisotropic behavior, the work of Paul and Heinze on an FeRh bilayer deposited on Re(0001) has shown that the EF-induced changes in the interaction parameters play an important role in defining the energy barriers for the EF-assisted writing and deleting of skyrmions [32]. Moreover, Desplat *et al.* have calculated how an external EF generates a DM interaction in an inversion-symmetric ultrathin film [33]. By performing atomistic simulations within the framework of an effective Heisenberg model with parameters derived from DFT, these authors have also shown how an EF pulse can result in the nucleation of a localized AF skyrmion around a magnetic defect.

The functionalities introduced by applying external EFs also open new prospects in the search for advanced magnetic materials that not only have a large magnetic anisotropy energy (MAE), and thus a particularly stable magnetization, but that are also tunable for fast and efficient magnetization reversal in the writing processes [20]. One expects in fact to design magnetic materials in which an external electric field is used to reduce the MAE when a spin reversal is intended, thus rendering the process faster and feasible at comparatively weaker magnetic fields or currents. Removing the EF after the writing process would then restore the full MAE, thus avoiding a superparamagnetic information loss. In this way, fast magnetization-reversal process could be achieved at relatively low-power consumption.

From a theoretical perspective the challenge remains to characterize and understand the microscopic origin of the EF dependence of the magnetic interactions and their anisotropy, which would be most useful for guiding material design and optimization. The EF manipulation of magnetic behaviors is particularly interesting in systems showing chiral magnetic order and chiral magnetic interactions. One of the main reasons is that chiral magnetic interactions are critically sensitive to the symmetry of the lattice structure and, more generally, to the form of the external potential $v_{\rm ext}(\boldsymbol{r})$ acting on the valence electrons responsible of magnetism. Indeed, if a system shows inversion symmetry [i.e., if $v_{\rm ext}(\boldsymbol{r}) = v_{\rm ext}(-\boldsymbol{r})$] one can show that the energies of a magnetic configuration and its mirror image are the same. In this case, a qualitative important mechanism of stabilizing noncollinear magnetic arrangement is absent because no energy can be gained by adopting a specific chirality. This problem has recently motivated a considerable experimental and theoretical research activity in relation to the formation, stabilization, and transport of localized noncollinear magnetic textures [29,31–33]. Applying an EF or attaching foreign atoms to a magnetic material opens remarkable opportunities of manipulating the magnetic behavior since these external sources break inversion symmetry, thus triggering the onset of DM couplings, which are responsible of chirality. The prospects of tuning the chirality of the magnetic order by EFs are particularly appealing in the case of low-dimensional systems and nanostructures (e.g., clusters, wires, and thin films) since screening is strongly limited in these systems due to their reduced coordination number and dimensionality.

The purpose of this paper is to demonstrate and quantify the possibilities of triggering and tuning chiral magnetic interactions in low-dimensional transition metal (TM) systems by means of EFs. To this aim a systematic study involving all $3d$, $4d$, and $5d$ freestanding TM dimers has been performed in the framework of DFT. The method used for the calculations is described in Sec. II. The results, presented in Sec. III, include an analysis of the EF dependence of the DM couplings, an account of the trends in the field-induced couplings as a function of band filling and across the different TM series, as well as an analysis of the dependence of the EF-induced DM couplings on the degree of noncollinearity between the local magnetic moments. Finally, the paper is closed in Sec. IV with a summary of our conclusions.

II. THEORETICAL METHODS

The effective pairwise interaction between the local magnetic moments $\boldsymbol{\mu}_i$ at the atoms i are obtained by expanding the total electronic energy to second order in the orientations of $\boldsymbol{\mu}_i$. The resulting approximation of the interaction energy takes the form of a classical spin Hamiltonian, which can be expressed, without loss of generality, as the sum of irreducible terms corresponding to different symmetries. One may thus distinguish isotropic, symmetric anisotropic, and antisymmetric anisotropic couplings [34,35]. The focus of this work is on the antisymmetric contribution known as the Dzyaloshinskii-Moriya interaction [36–39], which can be written in a geometrically transparent form as

$$H_{\rm DM} = \frac{1}{2}\sum_{i,j} \boldsymbol{D}_{ij} \cdot \left(\hat{\boldsymbol{\mu}}_i \times \hat{\boldsymbol{\mu}}_j\right), \tag{1}$$

where $\boldsymbol{D}_{ij} = -\boldsymbol{D}_{ji} \in \mathbb{R}^3$ is the DM pseudovector and $\hat{\boldsymbol{\mu}}_i = \boldsymbol{\mu}_i/\mu_i$ is the unit vector giving the orientation of the magnetic moment at atom i. Physically, $\boldsymbol{D}_{ij}$ defines the most favorable polarization plane and sense of rotation of $\boldsymbol{\mu}_i$ in noncollinear arrangements. Its magnitude determines the relative stability between magnetic configurations having opposite chiralities. The sign convention in Eq. (1) is such that the favored sense of rotation of the local magnetic moments, as we move from atom i to atom j, is the one in which $\hat{\boldsymbol{\mu}}_i$, $\hat{\boldsymbol{\mu}}_j$, and $\boldsymbol{D}_{ij}$ form a left-handed basis [i.e., $\boldsymbol{D}_{ij} \cdot (\hat{\boldsymbol{\mu}}_i \times \hat{\boldsymbol{\mu}}_j) < 0$]. For example, for a pair of atoms having local moments $\boldsymbol{\mu}_1$ and $\boldsymbol{\mu}_2$ located along the x axis, a DM vector $\boldsymbol{D}_{12}$ pointing along the positive z axis stabilizes the clockwise sense of rotation of the moments from $\boldsymbol{\mu}_1$ towards $\boldsymbol{\mu}_2$ within the xy plane relative to the counterclockwise sense of rotation. We denote here the left-handed or clockwise chirality with $-$ and the right-handed or counterclockwise one with $+$ (see Fig. 1).

As almost every magnetoanisotropic property, the strength of the DM vector $\boldsymbol{D}_{ij}$ depends critically on the details of the electronic structure and on the parameters that control it. This includes in particular the composition of the system, the strength of the spin-orbit (SO) interactions, and the local environment of the atoms [5,6,35,40,41]. In contrast, the direction of $\boldsymbol{D}_{ij}$ and the very presence of a nonvanishing DM coupling are largely defined by the point-group symmetry around the bond connecting the atoms i and j [37]. Consider two magnetic moments $\boldsymbol{\mu}_i$ and $\boldsymbol{\mu}_j$ located at $\boldsymbol{r}_i$ and $\boldsymbol{r}_j$, with $\boldsymbol{r}_{ij} = \boldsymbol{r}_j - \boldsymbol{r}_i$ being the vector connecting them and C the point bisecting the segment $\boldsymbol{r}_{ij}$. The following symmetry constraints

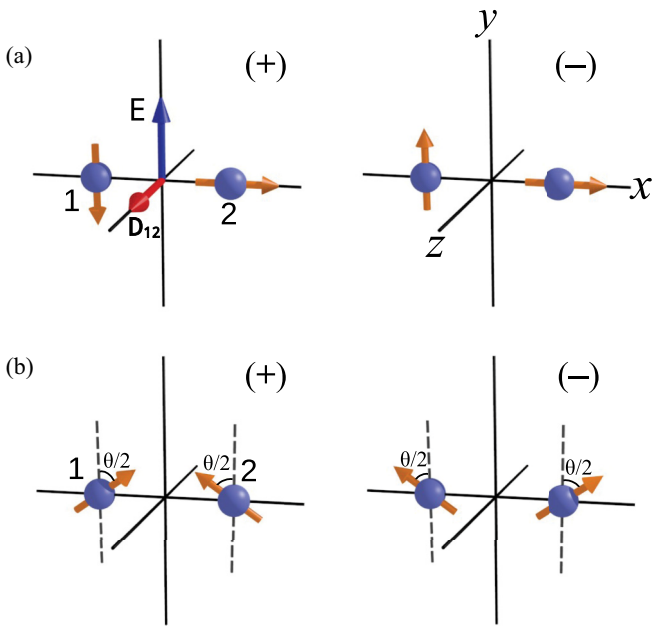

FIG. 1. Illustration of the noncollinear magnetic configurations used for calculating the electric field induced Dzyaloshinskii-Moriya (DM) interactions in transition metal dimers. The arrows at the atoms 1 and 2 indicate the orientation of the local magnetic moments $\boldsymbol{\mu}_i$ which turn in counterclockwise (+) or clockwise (−) sense within the xy plane as we move from 1 to 2: (a) maximal noncollinearity $\theta = \pi/2$ and (b) variable angle θ between the local moments. The positive directions of the electric field $\boldsymbol{E} = (0, E_y, 0)$ and DM vector $\boldsymbol{D}_{12} = (0, 0, D_{12}^z)$ are indicated.

on $\boldsymbol{D}_{ij}$ can then be derived by exploiting the pseudovector character of the local moments and the invariance of the interaction energy under symmetry transformations [37]: (i) If the system has an inversion symmetry with respect to C, then $\boldsymbol{D}_{ij} = 0$. (ii) If the system exhibits a mirror-symmetry plane that is perpendicular to $\boldsymbol{r}_{ij}$ and passes through C, then $\boldsymbol{D}_{ij}$ is perpendicular to $\boldsymbol{r}_{ij}$. And (iii) $\boldsymbol{D}_{ij}$ is perpendicular to any mirror-symmetry plane of the system that includes the bond $\boldsymbol{r}_{ij}$ connecting $\boldsymbol{r}_i$ and $\boldsymbol{r}_j$. Consequently, changing the symmetry of the system offers numerous possibilities of triggering DM couplings and thereby manipulating the stability of noncollinear magnetic arrangements with specific chiralities. For instance, in the case of one-dimensional chains, inversion symmetry implies $\boldsymbol{D}_{ij} = 0$. Therefore, breaking this symmetry, for example, by deposing the chains on a substrate, by decorating them with adatoms, or by applying an external electric field, would trigger finite DM couplings, thus resulting in a qualitative change of magnetic behavior [33,35]. Applying external electric fields is particularly interesting in this context since it offers a continuous reversible way of controlling the strength and orientation of the DM vectors.

The expression (1) for the DM interactions does not presuppose any specific microscopic mechanism responsible for these couplings. It simply encompasses the antisymmetric contributions to the two-body magnetic interactions, or quadratic dependence of the electronic energy, as a function of the orientation of the local magnetic moments $\boldsymbol{\mu}_i$ and $\boldsymbol{\mu}_j$. Therefore, it applies in principle to all intrinsic workings. However, the strength and orientation of $\boldsymbol{D}_{ij}$, as well as its geometric relation to the position and local environment of $\boldsymbol{\mu}_i$ and $\boldsymbol{\mu}_j$, do depend on the underlying electronic processes, which necessarily involve spin-orbit coupling. For example, in the derivations proposed by Moriya [37] and by Fert and Levy (FL) [3] an additional, typically nonmagnetic atom is required in the environment of $\boldsymbol{\mu}_i$ and $\boldsymbol{\mu}_j$ (e.g., an impurity or interface atom) in order to bring about the superexchange coupling or the scattering of the conduction electrons. In particular, the FL mechanism predicts that $\boldsymbol{D}_{ij}$ is proportional to $(\boldsymbol{r}_i - \boldsymbol{r}_0) \times (\boldsymbol{r}_j - \boldsymbol{r}_0)$, where $\boldsymbol{r}_0$ is the position of the mediating atom [3]. A different DM-coupling mechanism has been proposed in the *converse* spin-current model [42]. In this case, the presence of a permanent electric polarization, which can be driven, for example, by lattice distortions as in $BiFeO_3$ and which is essentially independent of the orientation of the magnetic moments, results in antisymmetric interactions between them. The corresponding DM vector $\boldsymbol{D}_{ij}$ bears here a very different relation to the local environment of the magnetic atoms i and j, as it is proportional to $\boldsymbol{p}_i \times \boldsymbol{r}_{ij}$, where $\boldsymbol{p}_i$ stands for the local electric polarization. In one- and two-dimensional systems, where the atoms and permanent electric dipoles lie on a common plane, it not possible to discern between these two mechanisms from the symmetry of $\boldsymbol{D}_{ij}$. However, in three-dimensional materials such a distinction is in principle possible. Indeed, a detailed analysis of the frozen-magnon dispersion relations in $BiFeO_3$ calculated with DFT has recently revealed the significance of the asymmetric exchange interactions induced by a converse spin-current effect over the structural asymmetry induced by the anionic octahedrons of the $BiFeO_3$ lattice [43]. Clearly, none of these mechanisms apply to freestanding homogeneous dimers since both a mediating atom and a preexisting permanent dipole are absent. As discussed in Sec. III, the EF-induced DM couplings that we observe can be qualitatively understood from the perspective of a magnetoelectric effect of a different nature, namely, in the frame of the spin-current model proposed by Katsura, Nagaosa, and Balatsky (KNB) [44]. According to this work, the spin-orbit interactions result in an electric polarization that is proportional to $\boldsymbol{r}_{ij} \times (\hat{\boldsymbol{\mu}}_i \times \hat{\boldsymbol{\mu}}_j)$ already in the absence of an external EF, provided that the magnetic order is noncollinear.

In this paper the DM interactions have been calculated by performing independent calculations of the electronic energy for different noncollinear magnetic configurations of the system. This is achieved by imposing constraints to the orientations of the local magnetic moments $\boldsymbol{\mu}_i$ at each atom i in the framework of Hohenberg-Kohn-Sham's DFT [45,46]. The DM vectors $\boldsymbol{D}_{ij}$ between atoms i and j are obtained by building appropriate total-energy differences between configurations having opposite chiralities. Figure 1 shows representative magnetic configurations of the dimers, in which the local moments are located in the xy plane and the chirality is counterclockwise (+) or clockwise (−). Once the corresponding total energies ε_+ and ε_- are obtained, the z component of the DM vector is given by

$$D_{12}^z = \frac{\varepsilon_+ - \varepsilon_-}{2\,\sin(\theta)}, \tag{2}$$

where θ is the angle between the local moments. Notice that the symmetric isotropic and anisotropic interactions

cancel out in $\Delta\varepsilon = \varepsilon_+ - \varepsilon_-$ because the magnetic configurations $+$ and $-$ are the chiral image of each other. In the limit of collinear local moments, D^z_{12} remains finite since $\Delta\varepsilon$ vanishes linearly as θ tends to 0 or π. If necessary, the other components of $\boldsymbol{D}_{ij}$ can be determined in an analogous way by considering similar magnetic configurations with local moments in the corresponding orthogonal planes. In the present case, D^z_{12} is the only nonvanishing component.

The DFT calculations have been done using the Vienna *ab initio* simulation package (VASP) [47,48]. The spin-polarized Kohn-Sham orbitals are expanded in an augmented plane-wave basis set, taking into account the interaction between valence electrons and ionic cores within the projector-augmented wave approximation [49]. Exchange and correlation effects are described by means of the Perdew-Burke-Ernzerhof parametrization of the generalized-gradient approximation [50]. While the orientations $\hat{\boldsymbol{\mu}}_i$ of the local moments are constrained, no restriction is imposed to their moduli. Thus, these degrees of freedom are optimized, which corresponds to the most stable solution of the Kohn-Sham equations for the given $\hat{\boldsymbol{\mu}}_i$ [51,52]. In practice, the sizes of the local magnetic moments are largely independent of the chirality of the magnetic configuration, although they may well depend on the angle between them.

The numerical convergence and stability of the calculations is ensured by considering fractional occupations of Kohn-Sham orbitals with a Gaussian smearing. The width of the Gaussian is progressively decreased in the range $0.9\ \text{eV} \geqslant \sigma \geqslant 0.01\ \text{eV}$ until the entropy contribution to the free energy is less than 10^{-3} eV/atom, often even practically zero. Concerning the expansion of the Kohn-Sham orbitals, a cutoff energy $E_{\max} = 500$ eV has been used for the plane-wave basis set. The self-consistent calculations are pursued until the change in the total energy between subsequent optimization steps is smaller than 10^{-6} eV. This is sufficient for our purposes, as we are interested in determining energy differences of the order of 10^{-4} eV or larger. The dimensions of the supercell are chosen to be large enough (at least 12 Å) so as to avoid any spurious interactions between the cluster images. As in any finite-cluster calculation only the gamma point is taken into account. The orientation of the local magnetic moments $\boldsymbol{\mu}_i$ is constrained along the directions $\hat{\boldsymbol{n}}_i$ corresponding to the considered noncollinear magnetic configuration by adding the penalty function to the Hohenberg-Kohn energy functional [53,54]. The local magnetic moments $\boldsymbol{\mu}_i$ are obtained by integrating the magnetization density $\boldsymbol{m}(\boldsymbol{r})$ within the Wigner-Seitz sphere Ω_i of atom i. Two methods are compared concerning the effects of spin-orbit interactions. The first and most rigorous one is a fully self-consistent treatment for each independent calculation with its specific chiral magnetic order. The second one is the force-theorem (FT) approximation, in which the spin-orbit interactions are incorporated *a posteriori*, once self-consistency at the scalar relativistic level has been reached [55]. By comparing these two approaches the relevance of a self-consistent treatment of SO interactions to the DM couplings can be quantified. In both cases the method implemented by Lebacq and Kresse is used [56,57].

III. RESULTS AND DISCUSSION

The general rules defining the orientation of $\boldsymbol{D}_{ij}$ with respect to the vector $\boldsymbol{r}_{ij} = \boldsymbol{r}_i - \boldsymbol{r}_j$ connecting the locations of a pair of magnetic moments $\boldsymbol{\mu}_i$ and $\boldsymbol{\mu}_j$ have been formulated by Moriya [37]. While these symmetry criteria certainly apply to the present situation, it is still instructive to consider the case of an external EF perpendicular to the dimer bond explicitly, by exploiting the pseudovector character of $\boldsymbol{D}_{ij}$. In fact, a reflection across the xy plane defined by $\boldsymbol{r}_{12} = (x_{12}, 0, 0)$ and the electric field $\boldsymbol{E} = (0, E_y, 0)$ leaves both $\boldsymbol{r}_{12}$ and $\boldsymbol{E}$ unchanged, while reversing the x and y components of $\boldsymbol{D}_{12}$ (see Fig. 1). Consequently, $D^x_{12} = D^y_{12} = 0$ for all E_y. Moreover, a reflection across the zx plane perpendicular to $\boldsymbol{E}$ reverses both E_y and D^z_{12}. Therefore, D^z_{12} is an odd function of E_y, i.e., $D^z_{12}(-E_y) = -D^z_{12}(E_y)$. For completeness, note that the reflection across the yz plane passing through the middle of the bond provides no further information since $\boldsymbol{E}$ is unchanged while $\boldsymbol{D}_{12}$ transforms to $(D^x_{21}, -D^y_{21}, -D^z_{21}) = (-D^x_{12}, D^y_{12}, D^z_{12})$. This confirms that $D^x_{12} = 0$ but yields no information on the other components.

In the following we focus on the nonvanishing component D^z_{12} of the DM vector. In Sec. III A the EF dependence of D^z_{12} is analyzed and the electric susceptibilities characterizing it are identified. The trends across the $3d$, $4d$, and $5d$ series are discussed in Sec. III B, giving emphasis to the microscopic origin of the observed $D^z_{12}(E)$. Complementary information on the local magnetic moments and SO energies is provided in Sec. III C. Finally, in Sec. III D we analyze how the EF-induced DM couplings depend on the degree of noncollinearity between the local magnetic moments.

A. Electric field dependence of the Dzyaloshinskii-Moriya interaction

In order to quantify the electric field induced DM coupling systematically and to identify the trends as a function of d-band filling and SOC strength we have performed density functional calculations for all $3d$, $4d$, and $5d$ dimers at the corresponding bulk nearest-neighbor (NN) distances. In Fig. 2 the EF dependence of the nonvanishing component D^z_{12} of the DM vector is shown for a few representative examples. Only positive values of E_y are considered since D^z_{12} is an odd function of E_y. One observes that the EF-induced DM couplings are largely dominated by a linear term, which is characterized by the first-order electric susceptibility of the DM interaction $\delta_{12} = \partial D^z_{12}/\partial E_y$ at zero field. The proportionality between D^z_{12} and E_y at low fields indicates that there are nonvanishing permanent dipole moments $\boldsymbol{p}^0_+$ and $\boldsymbol{p}^0_-$ in the noncollinear configurations $+$ and $-$, whose y component $p^{0,y}_{\pm}$ along the field depends on chirality. Aside from the linear term, a weaker cubic contribution to the field dependence of D^z_{12} is found, which can be characterized by the third-order susceptibility $\gamma_{12} = \partial^3 D^z_{12}/\partial E^3_y$ at zero field. In order to quantify δ_{12} and γ_{12} for the different elements, we have fitted the self-consistent (SC) density functional results (crosses) with functions of the form $D^z_{12}(E) = \delta_{12}E + \gamma_{12}E^3$. Figure 2 shows that these cubic expansions, given by the curves, describe remarkably well the EF dependence of the DM couplings. Concerning the role of SO interactions, it is

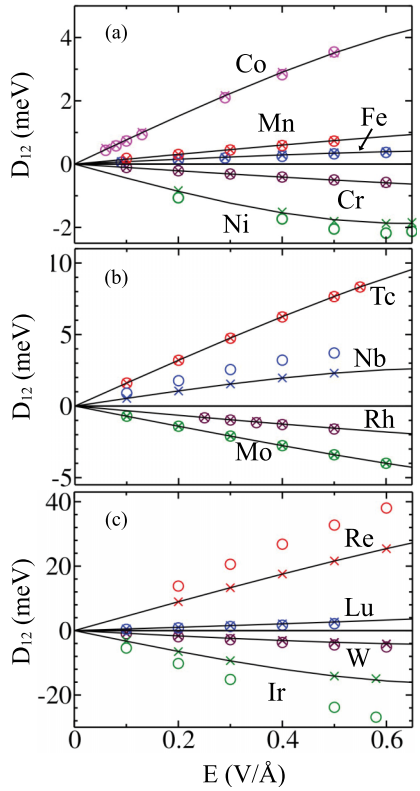

FIG. 2. Dzyaloshinskii-Moriya vector $\boldsymbol{D}_{12} = (0, 0, D_{12}^z)$ in transition metal dimers as a function of the applied electric field $\boldsymbol{E} = (0, E_y, 0)$. Results are shown for representative (a) $3d$, (b) $4d$, and (c) $5d$ transition metals, as obtained from self-consistent (crosses) and force-theorem (circles) calculations. The solid curves show the fit of the DFT results using the weak-field expansion $D_{12}^z(E) = -pE = -p_+^{(0)}E - \alpha_+^{(2)}E^3$, where $p_+^{(0)} = -p_-^{(0)}$ is the zero-field electric dipole moment and $\alpha_+^{(2)} = -\alpha_-^{(2)}$ the quadratic electric polarizability in the + configuration (see Fig. 1).

interesting to note that the results obtained using the simpler force-theorem (FT) approximation (circles) are in general very similar to the SC ones. The largest discrepancies are found for elements showing a particularly strong response to the field: Ni, Nb, and most notably the heavier Ir and Re. Nevertheless, even in these cases, the FT approximation is qualitatively correct. This indicates that, although SO interactions are central to the DM couplings, the redistributions of the spin-polarized electronic density resulting from them do not play an important role.

According to the symmetry rules governing antisymmetric magnetic interactions [37], a dimer shows no DM coupling in the absence of an external EF because the lattice structure has inversion symmetry. From this perspective, the DM vector induced by E_y can be regarded as the consequence of breaking the inversion symmetry and the C_∞ rotational symmetry around the bond axis. Electric fields along the dimer bond yield no DM coupling because of the remaining combination of C_∞ and σ_v symmetries [37]. However, a linear dependence of D_{12}^z on E_y, as shown in Fig. 2, is only possible when different permanent dipole moments $p_+^{0,y}$ and $p_-^{0,y}$ are already present in the magnetic configurations + and − in the absence of any external EF. In fact, it is the dependence of $p^{0,y}$ on the chirality of these magnetic configurations what explains the linear behavior of the DM coupling at finite fields [see Fig. 1(a)]. From this perspective, the microscopic origin of the EF-induced DM couplings is intrinsic to field-free dimer. It is rooted in the noncollinearity of the magnetic configurations + and −, and in the way in which the SO interactions are affected by their opposite chiralities. The EF serves then only as the means of rendering this chiral behavior apparent in the form of an antisymmetric interaction energy.

Symmetry arguments provide very useful information on the orientation of the dipole moments $\boldsymbol{p}_+^0$ and $\boldsymbol{p}_-^0$ resulting from SO interaction in the noncollinear magnetic configurations of the field-free dimers. One should first of all note that the total electronic density $n(\boldsymbol{r})$ is invariant upon time inversion. Therefore, the electric dipole moments are invariant upon reversing all local magnetic moments $\boldsymbol{\mu}_i$. Furthermore, concerning point-group symmetries, $\boldsymbol{p}^0$ transforms as a vector while $\boldsymbol{\mu}_i$ as a pseudovector. To be explicit, consider the configuration + shown in Fig. 1(a) and apply time inversion followed by a reflection across the xy plane. This combination of operations leaves the magnetic configuration unchanged. At the same time, the dipole moment $\boldsymbol{p}_+^0$ is unaffected by time inversion and its z component $p_+^{0,z}$ changes sign upon the xy reflections. Consequently, $p_+^{0,z} = 0$. Consider now the reflection of the configuration + across the zx plane, which leaves $\boldsymbol{\mu}_1$ unchanged and reverses $\boldsymbol{\mu}_2$, thus transforming the configuration + into the configuration −. In this case, $p^{0,y}$ changes sign while $p^{0,x}$ and $p^{0,z}$ remain unchanged. This implies that $p^{0,y}$ changes sign upon changing the chirality from + to − (i.e., $p_-^{0,y} = -p_+^{0,y}$) and that the other components are independent of chirality (i.e., $p_-^{0,z} = p_+^{0,z} = 0$ and $p_-^{0,x} = p_+^{0,x}$). One therefore concludes that the chirality of the dipole moment is given by $\Delta\boldsymbol{p}^0 = \boldsymbol{p}_+^0 - \boldsymbol{p}_-^0 = (0, 2p_+^{0,y}, 0)$. As a result, the dominant part of the EF-induced $\boldsymbol{D}_{12}$ arises from the dipole moments along the direction y or, more generally, along $\boldsymbol{r}_{12} \times (\boldsymbol{\mu}_1 \times \boldsymbol{\mu}_2)$ which is perpendicular to the vector connecting the atoms and lies within the plane spanned by $\boldsymbol{\mu}_1$ and $\boldsymbol{\mu}_2$. This component of $\boldsymbol{p}^0$ is consistent with the electric polarization derived in Ref. [44] from the spin current. Notice, however, that the dipole moment $p_+^{0,x}$ along the the bond connecting the atoms need not be zero since the noncollinear configurations + and − in Fig. 1(a) break the reflection symmetry across the plane passing through the middle of the dimer bond. In any case, the value of $p^{0,x}$ does not affect the DM coupling because $p_+^{0,x} = p_-^{0,x}$ [58].

In order to assess the importance of the EF-induced DM couplings quantitatively, it is useful to compare the results shown in Fig. 2 with the corresponding Heisenberg exchange couplings J_{12} typically found in dimers. These can be derived from the energy difference $J_{12} = (\varepsilon_{\uparrow\downarrow} - \varepsilon_{\uparrow\uparrow})/2$ between antiparallel and parallel alignment of the local moments. We focus on the dominant isotropic part of the exchange interaction and therefore average the spin-flip energies for orientations of the magnetic moments along the x, y, and z axes. Results for representative dimers are shown in Table I. As expected, J_{12} is orders of magnitude stronger than the spin-orbit driven D_{12}. The relative changes in J_{12} induced by an external electric field amount to a small percentage, at most 4% in the examples considered in Table I. However, in absolute values,

TABLE I. Symmetric isotropic exchange interaction J_{12} in transition metal dimers. Results are given in meV for the field-free case ($E_y = 0$) and for $E_y = 0.5$ V/Å (see Fig. 1). Positive (negative) values correspond to ferromagnetic (antiferromagnetic) couplings.

Dimer	$E_y = 0$	$E_y = 0.5$ V/Å
Fe_2	323	310
Ru_2	366	403
Os_2	281	258
Cr_2	−449	−447
Mo_2	−937	−934
W_2	−464	−462

the EF effect on J_{12} is similar and sometimes even larger that the EF-induced DM couplings (see also Fig. 2). Comparison with previous DFT calculations of the EF-induced modification of the Heisenberg exchange couplings for a freestanding Fe(001) monolayer and a Co monolayer on Pt(111) [30] indicates that in freestanding dimers J_{12} is significantly larger than the NN couplings in ultrathin films. This trend is consistent with the increasing stability of short-range ferromagnetic correlations observed in small Fe clusters as the cluster size decreases [59]. It can be ascribed to the reduction of the effective d-band width and the concomitant enhancement of the local magnetic moments and exchange splittings as the coordination number is reduced. Concerning the EF-induced modifications of J_{12}, the dimers often show a reduction (see Table I) whereas for the Fe monolayer an increase of the NN coupling has been reported [30]. Quantitatively, the absolute changes found in the dimers also tend to be stronger, which could be related to poorer screening.

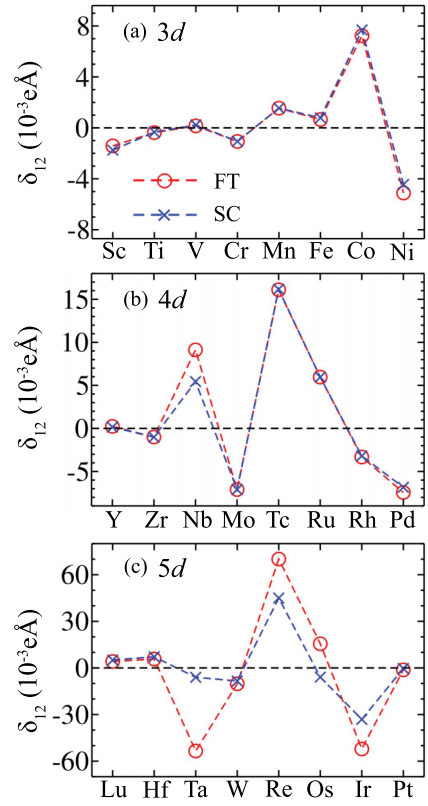

FIG. 3. First-order electric susceptibility of the Dzyaloshinskii-Moriya interaction $\delta_{12} = \partial D_{12}^z/\partial E = p_+^{(0,z)}$ at zero field in (a) $3d$, (b) $4d$, and (c) $5d$ transition metal dimers. Self-consistent (SC, crosses) and force-theorem results (FT, circles) are compared. The lines connecting the points are a guide to the eye. See also Fig. 2.

B. Electric susceptibilities of the DM interaction

The previous section has shown that the EF dependence of the DM interaction in TM dimers is very well described by the cubic expansion $D_{12}^z(E) = -p_+^{(0)}E - \alpha_+^{(2)}E^3$, where $p_+^{(0)} = -p_-^{(0)}$ is the electric dipole moment and $\alpha_+^{(2)} = -\alpha_-^{(2)}$ is the second-order electric polarizability at zero field in the magnetic configuration + [see Fig. 1(a)]. It is therefore meaningful to characterize the trends across the TM series by considering the zero-field electric susceptibility of the DM interaction $\delta_{12} = \partial D_{12}^z/\partial E = p_+^{(0,z)}$ and the third-order susceptibility $\gamma_{12} = \partial^3 D_{12}^z/\partial E^3$. The results for these properties are given in Figs. 3 and 4, respectively [60].

The coefficient δ_{12} of the dominant linear dependence of D_{12}^z on the EF strength coincides with the permanent dipole moment $p_+^{(0,z)}$ in the configuration + since at zero field $p_-^{(0,z)} = -p_+^{(0,z)}$. In Fig. 3 one observes that δ_{12} depends strongly on d-band filling, showing remarkable oscillations and changes of sign across the TM series. This reflects the known strong sensitivity of SO effects on the details of the electronic structure. The amplitude of the oscillations and typical values of δ_{12} increase as we move from the lighter $3d$ to the heavier $5d$ elements, in accordance with the corresponding increase of the SO coupling strength. The variety of behaviors defies easy generalizations. For example, in the $3d$ series, δ_{12} is particularly small, showing weak oscillations as long as the band filling is lower or equal to that of Fe. In contrast, at the end of the series, the response to the electric is not only much stronger but it also shows opposite signs in Co and Ni. Comparison with previous DFT calculations of the magnetoelectric couplings for freestanding Mn, Fe, Co, and Ni monolayers [33] confirms that the EF-induced DM vectors in the dimers follow the same local-symmetry rules as in these inversion-symmetric extended 2D systems (i.e., $\boldsymbol{D}_{ij} \propto \boldsymbol{E} \times \hat{\boldsymbol{r}}_{ij}$). However, the quantitative differences are very important. The DM couplings per unit electric field δ_{12} in $3d$-TM dimers are found to be typically two orders of magnitude stronger than the results reported in Ref. [33]. This trend is consistent with the enhancement of the MAE in small TM clusters as the local coordination number is reduced [61]. The dependence of the DM interactions on external EFs has also been theoretically investigated for deposited thin films which lack inversion symmetry, and therefore show significant DM couplings already in the absence of a field. In the case of an FeRh bilayer on Re(0001) one finds that the DM coupling changes by 0.07 meV upon varying the EF from −0.5 to 0.5 V/Å [32]. This value is significantly smaller than our dimer results. For example, the corresponding change in D_{12}^z for Fe_2 is approximately 0.7 meV (see Fig. 2).

In the $4d$ series the oscillations of δ_{12} as a function of the number of d electrons are significantly stronger than in the $3d$ series. Nevertheless, one observes that most isoelectronic

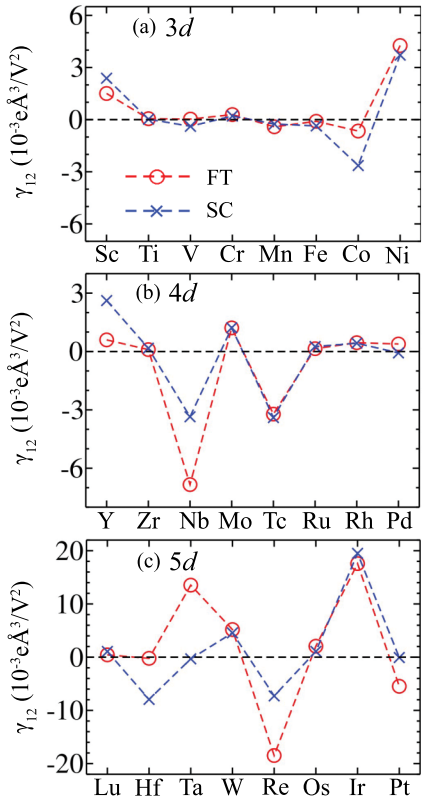

FIG. 4. Third-order electric susceptibility of the Dzyaloshinskii-Moriya interaction $\gamma_{12} = \partial^3 D_{12}^z / \partial E^3$ at zero field in (a) $3d$, (b) $4d$, and (c) $5d$ transition metal dimers. Self-consistent (SC, crosses) and force-theorem results (FT, circles) are compared. The lines connecting the points are a guide to the eye. See also Fig. 2.

$3d$ and $4d$ elements follow similar trends. Compare the oscillations of δ_{12} upon going from Ti to Fe in Fig. 3(a) with those found from Zr to Ru in Fig. 3(b). And yet, δ_{12} in Co and Rh have opposite signs, thus breaking the common trend. In the $5d$ series a comparable increase of the amplitude of the oscillations is observed relative to the $4d$ series [cf. Figs. 3(b) and 3(c)]. While some isoelectronic $4d$ and $5d$ dimers show a similar behavior (e.g., Tc and Re or Rh and Ir), several others contrast (e.g., Nb and Ta, Mo and W, or Pd and Pt).

Further information of the magnetic response to the EF is provided by the zero-field third-order electric susceptibility of the DM coupling γ_{12}, which measures the deviations of D_{12}^z from linearity (see also Fig. 2). In Fig. 4 one observes either that γ_{12} is quite small or that its sign is opposite to that of δ_{12}. The former corresponds to a nearly linear behavior, while the latter reflects a tendency to saturation. Accordingly, relative large absolute values of δ_{12} correlate with significant γ_{12}. As expected, γ_{12} is generally larger in the $5d$ elements, which are subject to stronger SO coupling. In addition, one observes that the SC and FT treatments of SO interactions yield almost always very similar results, as in Fig. 2. The discrepancies, even if not significant qualitatively, are more noticeable in the heavier elements and in the more subtle γ_{12} (see Figs. 3 and 4). In particular, the sign of δ_{12} and γ_{12} obtained in FT and SC calculations is almost always the same.

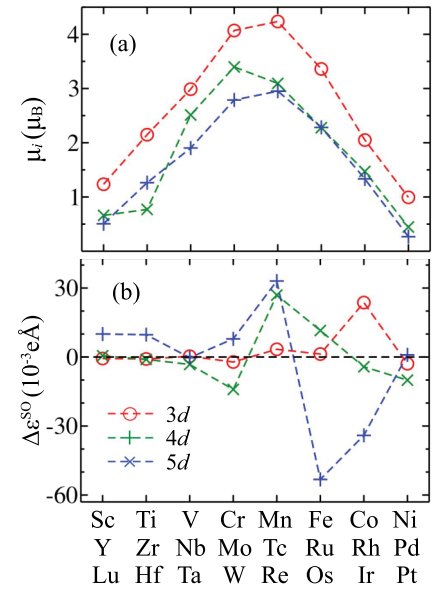

FIG. 5. (a) Local magnetic moments μ_i and (b) chirality of the spin-orbit energy per unit electric field $\Delta\varepsilon^{SO} = (\varepsilon_+^{SO} - \varepsilon_-^{SO})/E_y$ in TM dimers with bulk NN distances, as derived from independent self-consistent calculations. The lines connecting the points are a guide to the eye [60].

C. Local moments and spin-orbit energies

To gain a further insight into possible correlations between the EF-induced DM interactions and other important magnetic properties it is useful to analyze the trends in the local magnetic moments μ_i and in the average SO energies $\varepsilon_\pm^{SO}$ across the TM series. In Fig. 5(a) one observes that below half-band filling μ_i increases almost linearly with increasing number of d electrons n_d, reaching a maximum for Cr, Mn and the isoelectronic $4d$ and $5d$ elements. Beyond half-band filling μ_i decreases as the number of d holes is reduced towards the end of the series. This corresponds to nearly saturated moments, which can be qualitatively understood by recalling that the d-band width is strongly reduced in systems having such a small local coordination number [62]. The structureless dependence of μ_i as a function of n_d contrasts with the strong oscillations found in δ_{12} and γ_{12} (see Figs. 3 and 4). No correlation between the strength of the EF-induced DM coupling and the size of the local magnetic moments is observed. This behavior differs from the one observed at $3d$-$5d$ interfaces, where the DM interaction was found to follow Hund's first rule [7].

In Fig. 5(b) results are shown for the chirality of the SO energy per unit electric field, which is given by $\Delta\varepsilon^{SO} = (\varepsilon_+^{SO} - \varepsilon_-^{SO})/E_y$. One observes a strong band-filling dependence with oscillations whose amplitudes increase as we move from the $3d$ to the $5d$ series. Given the strong dependencies of $\Delta\varepsilon^{SO}$ and δ_{12} on n_d, it is interesting to compare them in order to identify possible correlations between these properties. For instance, in the $3d$ series, $\Delta\varepsilon^{SO}$ displays weak oscillations for band fillings up to Fe, followed by a strong increase for Co, and a change of sign for Ni. These trends agree qualitatively with the results on δ_{12} shown in Fig. 3(a). Furthermore, $\Delta\varepsilon^{SO}$ also reproduces most of the nontrivial differences between

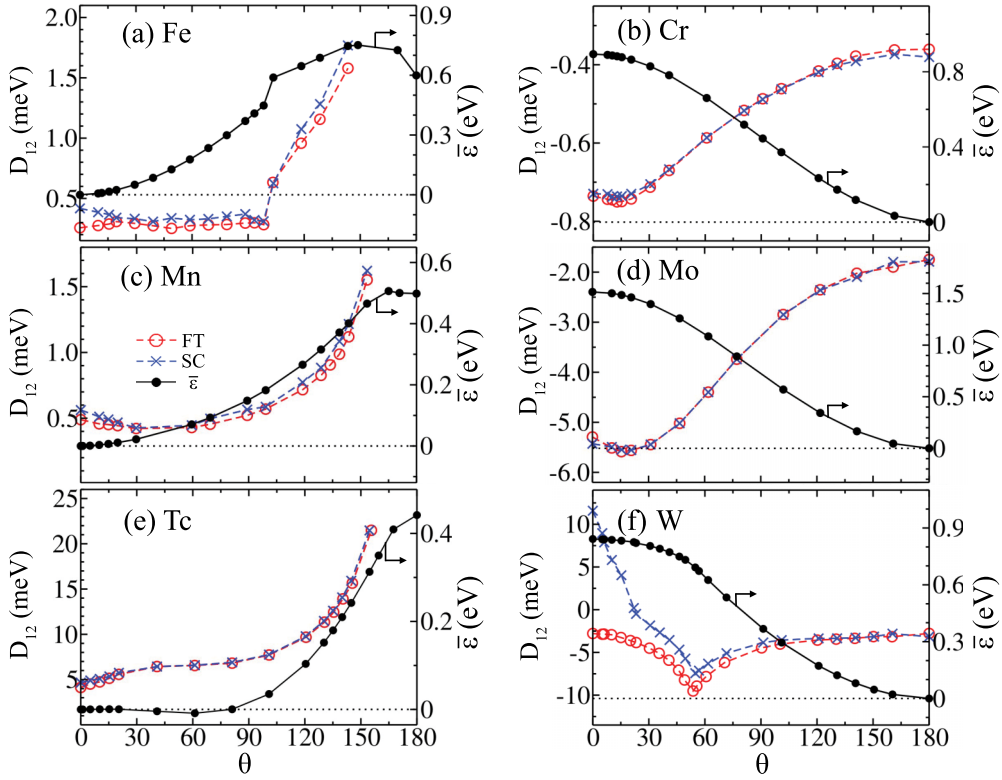

FIG. 6. Dzyaloshinskii-Moriya interaction D_{12}^{z} as a function of the angle θ between the local magnetic moments at the atoms 1 and 2 in representative TM dimers having bulk NN distances and subject to an external electric field $E_y = 0.5$ V/Å [see Eq. (2) and Fig. 1(b)]. The results are derived from independent self-consistent calculations (SC, crosses) or by using the force-theorem approximation (FT, open circles) [63]. The corresponding increase of the average energy $\bar{\varepsilon} = [\varepsilon_+(\theta) + \varepsilon_+(\theta)]/2$ relative to the ground state is given by the solid curves with dots.

the $3d$ and $4d$ values of δ_{12}. Indeed, the oscillations and changes of sign in $\Delta\varepsilon^{\mathrm{SO}}$ from Mo to Pd are very similar to the trends observed in δ_{12}. However, in the case of Nb, the results on $\Delta\varepsilon^{\mathrm{SO}}$ disagree qualitatively with the susceptibility of the DM coupling δ_{12} since their signs are opposite. Also in the $5d$ series both similarities and discrepancies are found. For example, the Re (Ir) dimer has a relatively strong positive (negative) $\Delta\varepsilon^{\mathrm{SO}}$, which is consistent with the relatively large positive (negative) δ_{12}. However, $\Delta\varepsilon^{\mathrm{SO}}$ is strongest and negative for Os, although the corresponding δ_{12} is relatively small [cf. Figs. 3(c) and 5(b)]. While these results confirm that the average SO energy represents an important, most often dominant contribution to the EF-induced DM interactions, they also show that other dimer-specific properties, such as the electric polarizability, the redistributions of the spin and orbital polarized density, and the details of the electronic structure, can also play an important role.

D. DM interaction and degree of noncollinearity

The DM interactions discussed in the previous sections have been derived from electronic calculations on the magnetic configurations with chiralities + and − illustrated in Fig. 1(a), in which the interacting local magnetic moments $\boldsymbol{\mu}_1$ and $\boldsymbol{\mu}_2$ are orthogonal to each other. These magnetic arrangements are particularly interesting from the perspective of anisotropic antisymmetric interactions because they represent the strongest degree of noncollinearity, halfway between the ferromagnetic and antiferromagnetic alignments. Nevertheless, in many situations of practical interest, the angle between the interacting nearby moments differs strongly from $\pi/2$, particularly when the noncollinearity is the result of the competition between relatively strong exchange couplings and much weak anisotropy energies, for example, in domain walls and skyrmions. It is therefore of considerable interest to investigate the dependence of the effective DM couplings $\boldsymbol{D}_{ij}$ on the degree of noncollinearity of the magnetic order. To this aim we consider the magnetic configurations illustrated in Fig. 1(b) and determine D_{12}^{z} from Eq. (2) by performing self-consistent and force-theorem total-energy calculations within the framework of DFT, by varying systematically the angle θ between the local moments $\boldsymbol{\mu}_1$ and $\boldsymbol{\mu}_2$.

The dependence of D_{12}^{z} as a function of θ is shown in Fig. 6 for representative TM dimers subject to an external electric field $E_y = 0.5$ V/Å. This figure also includes the average ground-state energy $\bar{\varepsilon} = [\varepsilon_+(\theta) + \varepsilon_+(\theta)]/2$, from which the ground-state order (ferromagnetic, noncollinear, or antiferromagnetic) and its stability can be inferred. The corresponding local magnetic moments μ_i are given in Fig. 7. A remarkable dependence of the EF-induced DM interactions on the degree of noncollinearity between the local moments is revealed. If one considers the complete range of relative orientations of $\boldsymbol{\mu}_i$, from parallel to antiparallel, the changes in D_{12}^{z} are very significant indeed [63]. This is not surprising since forcing a ferromagnetic system to be antiferromagnetic, or vice versa, implies a drastic change in its electronic structure, which

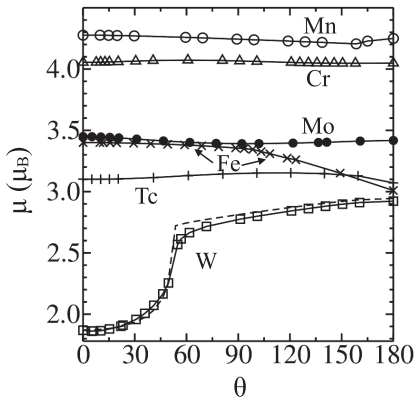

FIG. 7. Local magnetic moments μ_i at the atoms $i = 1$ and 2 in representative TM dimers as a function of the angle θ between them [see Fig. 1(b)]. The results are obtained from self-consistent calculations (SC, full curves with symbols) or force-theorem calculations (FT, dashed curve) for an external electric field $E_y = 0.5$ V/Å. Except for W, the FT results are indistinguishable from the SC ones on the scale of the plot. The corresponding DM couplings and average energies are shown in Fig. 6.

definitely affects the details of the SO interactions and the anisotropic properties derived from it. Nevertheless, the sign of D^z_{12} and thus the favored chirality are in most cases preserved, even when the angle between local moments is far from the equilibrium one. Quantitatively, $|D^z_{12}|$ tends to increase for the most part as θ deviates from the value yielding the lowest average energy $\bar{\varepsilon}$ (see Fig. 6).

In usual applications of effective classical spin models it is implicitly assumed that D^z_{12} depends weakly on θ, at least as long as the noncollinear orientation of the local moments is not too far from the ground-state order, i.e., small (large) θ for ferromagnetic (antiferromagnetic) systems. Our calculations show that, in the ferromagnetic dimers Fe_2, Mn_2, and Tc_2 this assumption is justified. In fact, in these cases, D^z_{12} is not far from its ground-state value, even for the orthogonal configuration ($\theta \simeq 90^\circ$). In antiferromagnetic W_2, the DM coupling is enhanced by 10% (22%) when θ varies from 180° to about 115° (90°). However, in Cr_2 and Mo_2, which are also antiferromagnetic, the dependence of D^z_{12} on the degree of noncollinearity is clearly stronger. For example, in Cr_2 (Mo_2) we find that D^z_{12} changes by 10% with respect to the value close to antiparallel alignment already when $\theta \simeq 130^\circ$ ($\theta \simeq 135^\circ$) reaching a 30% (75%) change in the orthogonal configuration. These modifications of D^z_{12} reflect important deviations of the DM interaction energy from the proportionality to $\sin(\theta)$. In the case of Cr and Mo, they cannot be ascribed to strong changes in the local magnetic moments μ_i, which remain remarkably stable for all θ, as shown in Fig. 7. Significant changes in μ_i are found in W_2 for $\theta < 60^\circ$ and to a lesser extent in Fe_2 for $\theta > 90^\circ$, in both cases far from the ground-state order. They are the evidence of changes in the electronic structure which correlate with changes in the behavior of both D^z_{12} and $\bar{\varepsilon}$ (see Fig. 6). In sum, the above results support the assumption of transferability of the DM couplings in effective spin models only within a restricted degree of noncollinearity. Moreover, they also reveal some of the quantitative limitations of unrestricted applications.

IV. CONCLUSION

Symmetry considerations show that an external EF can induce antisymmetric DM interactions between local magnetic moments $\boldsymbol{\mu}_i$ and $\boldsymbol{\mu}_j$ whose local environment exhibits inversion symmetry in the absence of a field. They also predict the orientation of the DM-coupling vector $\boldsymbol{D}_{ij}$ as the one perpendicular to the electric field $\boldsymbol{E}$ and the line connecting the moment locations. And still, they provide no information on the importance of the EF-induced couplings, their material dependence, or their microscopic origin. In this work the concrete possibilities of triggering and manipulating the DM couplings in low-dimension systems by electric means have been demonstrated by performing a systematic electronic study of all TM dimers in the framework of DFT. The dependence of the nonvanishing DM-vector component D^z_{ij} on the electric field E has been shown to be nearly linear for $|E| \leqslant 0.6$ V/Å, the third-order corrections having mostly a minor importance. The trends across the TM series have been characterized by computing the zero-field first-order electric susceptibility of the DM couplings δ_{ij}, as well as the corresponding third-order susceptibility γ_{ij}, and analyzing them as functions of the d-band filling. The microscopic source of the EF-induced antisymmetric magnetic interactions has been shown to reside in the permanent electric dipole moments $\boldsymbol{p}^0$ that field-free dimers develop as a result of SO coupling when their local magnetic moments adopt noncollinear configurations. The symmetry rules governing $\boldsymbol{p}^0$ and its dependence on the chirality of the underlying magnetic configuration have been derived. Furthermore, interesting correlations between δ_{ij} and the chirality of the spin-orbit energy have been displayed.

Phenomenological spin models are remarkably useful in order to investigate the physics of magnetic materials showing anisotropic competing interactions. Not only their transparency is most appealing from a theoretical perspective. but also their simplicity is extremely interesting since it allows a thorough exploration of the complex energy landscapes of these systems, as well as simulations of dynamical processes. Still, the determination of material-specific interaction parameter must rely on theoretical methods that take into account how the electronic structure and the resulting interaction energies depend on the local environment of the atoms and on the orientations of the magnetic moments. Moreover, once the effective interactions have been derived from electronic calculations for a given set of the magnetic arrangements, as in this work, their transferability to other magnetic orders should be verified. Investigations of the dependence of the DM couplings on the degree of noncollinearity of the magnetic order are therefore important. To this aim the EF-induced DM couplings have been calculated within DFT by varying the angle θ between the local moments. We have shown that changes in the effective DM-coupling vector $\boldsymbol{D}_{ij}$ are in general important when θ differs strongly from its ground-state value (i.e., $\theta = 0$ for ferromagnetic dimers and $\theta = 180^\circ$ for antiferromagnetic ones). The transferability of $\boldsymbol{D}_{ij}$ is thus restricted to a limited degree of noncollinearity. These results reflect the impossibility of casting the full complexity of the quantum many-body problem of strongly interacting delocalized d electrons into a classical spin model. Nonetheless, it is quite encouraging

to see that the changes in D_{12}^{z} are small for values of θ that deviate from the ground state by as much as 30° in the most complicated cases (Cr and Mo dimers) or even by 90° in other examples (Mn, Fe, and Tc dimers). With these restrictions in mind, the effective magnetic interactions derived from electronic calculations are reasonably transferable and well suited for simulations in the framework of phenomenological spin models involving competing interactions and complex noncollinear orders, particularly when the focus is on the low-lying states, where the magnetic arrangements do not deviate strongly from the ground state.

The element-specific behaviors and general tendencies derived in this work, for example, as a function of d-band filling or across different TM series, are expected to be useful as a guide for further theoretical investigations of the DM interactions in other interesting low-dimensional systems. In this context one should mention small TM clusters, in which different local environments coexist and influence each other, and one-dimensional chains, where both extended and localized noncollinear magnetic orders can be anticipated. Furthermore, it would be interesting to extend and compare this study with investigations on deposited dimers and alloy clusters, where different microscopic mechanisms leading to antisymmetric exchange couplings are expected to come into play.

ACKNOWLEDGMENTS

It is a pleasure to thank Dr. S. Riemer for helpful discussions and suggestions at the early stages of this work. Computer resources provided by the CSC of the University of Frankfurt and by the IT Service Center of the University of Kassel are gratefully acknowledged.

[1] R. E. Camley and K. L. Livesey, Consequences of the Dzyaloshinskii-Moriya interaction, Surf. Sci. Rep. **78**, 100605 (2023).

[2] H. Yang, J. Liang, and Q. Cui, First-principles calculations for Dzyaloshinskii–Moriya interaction, Nat. Rev. Phys. **5**, 43 (2023).

[3] A. Fert and P. M. Levy, Role of anisotropic exchange interactions in determining the properties of spin-glasses, Phys. Rev. Lett. **44**, 1538 (1980).

[4] M. Bode, M. Heide, K. von Bergmann, P. Ferriani, S. Heinze, G. Bihlmayer, A. Kubetzka, O. Pietzsch, S. Blügel, and R. Wiesendanger, Chiral magnetic order at surfaces driven by inversion asymmetry, Nature (London) **447**, 190 (2007).

[5] V. Kashid, T. Schena, B. Zimmermann, Y. Mokrousov, S. Blügel, V. Shah, and H. G. Salunke, Dzyaloshinskii-Moriya interaction and chiral magnetism in 3d–5d zigzag chains: Tight-binding model and *ab initio* calculations, Phys. Rev. B **90**, 054412 (2014).

[6] H. Yang, A. Thiaville, S. Rohart, A. Fert, and M. Chshiev, Anatomy of Dzyaloshinskii-Moriya interaction at Co/Pt interfaces, Phys. Rev. Lett. **115**, 267210 (2015).

[7] A. Belabbes, G. Bihlmayer, F. Bechstedt, S. Blügel, and A. Manchon, Hund's rule-driven Dzyaloshinskii-Moriya interaction at 3d−5d interfaces, Phys. Rev. Lett. **117**, 247202 (2016).

[8] B. Schweflinghaus, B. Zimmermann, M. Heide, G. Bihlmayer, and S. Blügel, Role of Dzyaloshinskii-Moriya interaction for magnetism in transition-metal chains at Pt step edges, Phys. Rev. B **94**, 024403 (2016).

[9] A. Deka, B. Rana, R. Anami, K. Miura, H. Takahashi, Y. C. Otani, and Y. Fukuma, Electric-field control of interfacial in-plane magnetic anisotropy in CoFeB/MgO junctions, Phys. Rev. B **101**, 174405 (2020).

[10] A. Rajanikanth, T. Hauet, F. Montaigne, S. Mangin, and S. Andrieu, Magnetic anisotropy modified by electric field in V/Fe/MgO(001)/Fe epitaxial magnetic tunnel junction, Appl. Phys. Lett. **103**, 062402 (2013).

[11] D. Preziosi, M. Alexe, D. Hesse, and M. Salluzzo, Electric-field control of the orbital occupancy and magnetic moment of a transition-metal oxide, Phys. Rev. Lett. **115**, 157401 (2015).

[12] W. Zhang, H. Zhong, R. Zang, Y. Zhang, S. Yu, G. Han, G. L. Liu, S. S. Yan, S. Kang, and L. M. Mei, Electrical field enhanced interfacial Dzyaloshinskii-Moriya interaction in MgO/Fe/Pt system, Appl. Phys. Lett. **113**, 122406 (2018).

[13] T. Koyama, Y. Nakatani, J. Ieda, and D. Chiba, Electric field control of magnetic domain wall motion via modulation of the Dzyaloshinskii-Moriya interaction, Sci. Adv. **4**, eaav0265 (2018).

[14] M. Rafique, A. Herklotz, K. Dörr, and S. Manzoor, Reversible electric-field-driven magnetization in a columnar nanocomposite film, Thin Solid Films **685**, 47 (2019).

[15] Y. Ba, S. Zhuang, Y. Zhang, Y. Wang, Y. Gao, H. Zhou, M. Chen, W. Sun, Q. Liu, G. Chai, J. Ma, Y. Zhang, H. Tian, H. Du, W. Jiang, C. Nan, J.-M. Hu, and Y. Zhao, Electric-field control of skyrmions in multiferroic heterostructure via magnetoelectric coupling, Nat. Commun. **12**, 322 (2021).

[16] H. Terada, S. Ohya, L. D. Ahn, Y. Iwasa, and M. Tanada, Magnetic anisotropy control by applying an electric field to the side surface of ferromagnetic films, Sci. Rep. **7**, 5618 (2017).

[17] H. Mizuno, T. Moriyama, K. Tanaka, M. Kawaguchi, T. Koyama, D. Chiba, and T. Ono, Electric field effect on spectroscopic g-factor and magnetic anisotropy in a Pt/Co/Mgo ultrathin film, Jpn. J. Appl. Phys. **61**, 103001 (2022).

[18] B. Dai, D. Wu, S. A. Razavi, S. Xu, H. He, Q. Shu, M. Jackson, F. Mahfouzi, H. Huang, Q. Pan, Y. Cheng, T. Qu, T. Wang, L. Tai, K. Wong, N. Kioussis, and K. L. Wang, Electric field manipulation of spin chirality and skyrmion dynamic, Sci. Adv. **9**, eade6836 (2023).

[19] X. Xue, Z. Zhou, B. Peng, M. Zhu, Y. Zhang, W. Ren, T. Ren, X. Yang, T. Nan, N. X. Sun, and M. Liu, Electric field induced reversible 180° magnetization switching through tuning of interfacial exchange bias along magnetic easy-axis in multiferroic laminates, Sci. Rep. **5**, 16480 (2015).

[20] A. Sonntag, J. Hermenau, A. Schlenhoff, J. Friedlein, S. Krause, and R. Wiesendanger, Electric-field-induced magnetic anisotropy in a nanomagnet investigated on the atomic scale, Phys. Rev. Lett. **112**, 017204 (2014).

[21] A. A. Khajetoorians, M. Steinbrecher, M. Ternes, M. Bouhassoune, M. dos Santos Dias, S. Lounis, J. Wiebe, and

R. Wiesendanger, Tailoring the chiral magnetic interaction between two individual atoms, Nat. Commun. **7**, 10620 (2016).
[22] K. Nakamura, R. Shimabukuro, Y. Fujiwara, T. Akiyama, T. Ito, and A. J. Freeman, Giant modification of the magnetocrystalline anisotropy in transition-metal monolayers by an external electric field, Phys. Rev. Lett. **102**, 187201 (2009).
[23] J. Hu and R. Wu, Control of the magnetism and magnetic anisotropy of a single-molecule magnet with an electric field, Phys. Rev. Lett. **110**, 097202 (2013).
[24] M. Tsujikawa and T. Oda, Finite electric field effects in the large perpendicular magnetic anisotropy surface Pt/Fe/Pt(001): A first-principles study, Phys. Rev. Lett. **102**, 247203 (2009).
[25] M. Tanveer, J. Dorantes-Dávila, and G. M. Pastor, Reversible electric-field manipulation of the adsorption morphology and magnetic anisotropy of small Fe and Co clusters on graphene, Phys. Rev. B **96**, 224413 (2017).
[26] B. Pradines, B. Cahier, N. Suaud, and N. Guihéry, Impact of the electric field on isotropic and anisotropic spin Hamiltonian parameters, J. Chem. Phys. **157**, 204308 (2022).
[27] N. N. Negulyaev, V. S. Stepanyuk, W. Hergert, and J. Kirschner, Electric field as a switching tool for magnetic states in atomic-scale nanostructures, Phys. Rev. Lett. **106**, 037202 (2011).
[28] E. Torun, H. Sahin, C. Bacaksiz, R. T. Senger, and F. M. Peeters, Tuning the magnetic anisotropy in single-layer crystal structures, Phys. Rev. B **92**, 104407 (2015).
[29] X. Z. Yu, Y. Onose, N. Kanazawa, J. H. Park, J. H. Han, Y. Matsui, N. Nagaosa, and Y. Tokura, Real-space observation of a two-dimensional skyrmion crystal, Nature (London) **465**, 901 (2010).
[30] M. Oba, K. Nakamura, T. Akiyama, T. Ito, M. Weinert, and A. J. Freeman, Electric-field-induced modification of the magnon energy, exchange interaction, and Curie temperature of transition-metal thin films, Phys. Rev. Lett. **114**, 107202 (2015).
[31] M. A. Goerzen, S. von Malottki, G. J. Kwiatkowski, P. F. Bessarab, and S. Heinze, Atomistic spin simulations of electric-field-assisted nucleation and annihilation of magnetic skyrmions in Pd/Fe/Ir(111), Phys. Rev. B **105**, 214435 (2022).
[32] S. Paul and S. Heinze, Electric-field driven stability control of skyrmions in an ultrathin transition-metal film, npj Comput. Mater. **8**, 105 (2022).
[33] L. Desplat, S. Meyer, J. Bouaziz, P. M. Buhl, S. Lounis, B. Dupé, and P.-A. Hervieux, Mechanism for ultrafast electric-field driven skyrmion nucleation, Phys. Rev. B **104**, L060409 (2021).
[34] L. Udvardi, L. Szunyogh, K. Palotás, and P. Weinberger, First-principles relativistic study of spin waves in thin magnetic films, Phys. Rev. B **68**, 104436 (2003).
[35] B. Jang, S. Riemer, and G. M. Pastor, Chiral magnetic interactions in small Fe clusters triggered by symmetry-breaking adatoms, Symmetry **15**, 397 (2023).
[36] I. Dzyaloshinsky, A thermodynamic theory of "weak" ferromagnetism of antiferromagnetics, J. Phys. Chem. Solids **4**, 241 (1958).
[37] T. Moriya, Anisotropic superexchange interaction and weak ferromagnetism, Phys. Rev. **120**, 91 (1960).
[38] F. Keffer, Moriya interaction and the problem of the spin arrangements in βMnS, Phys. Rev. **126**, 896 (1962).
[39] T. Moriya, New Mechanism of anisotropic superexchange interaction, Phys. Rev. Lett. **4**, 228 (1960).
[40] V. E. Dmitrienko, E. N. Ovchinnikova, S. P. Collins, G. Nisbet, G. Beutier, Y. O. Kvashnin, V. V. Mazurenko, A. I. Lichtenstein, and M. I. Katsnelson, Measuring the Dzyaloshinskii–Moriya interaction in a weak ferromagnet, Nat. Phys. **10**, 202 (2014).
[41] H. Yang, O. Boulle, V. Cros, A. Fert, and M. Chshiev, Controlling Dzyaloshinskii-Moriya interaction via chirality dependent atomic-layer stacking, insulator capping and electric field, Sci. Rep. **8**, 12356 (2018).
[42] D. Rahmedov, D. Wang, J. Íñiguez, and L. Bellaiche, Magnetic cycloid of $BiFeO_3$ from atomistic simulations, Phys. Rev. Lett. **109**, 037207 (2012).
[43] S. Meyer, B. Xu, M. J. Verstraete, L. Bellaiche, and B. Dupé, Spin-current driven dzyaloshinskii-moriya interaction in multiferroic $BiFeO_3$ from first principles, Phys. Rev. B **108**, 024403 (2023).
[44] H. Katsura, N. Nagaosa, and A. V. Balatsky, Spin current and magnetoelectric effect in noncollinear magnets, Phys. Rev. Lett. **95**, 057205 (2005).
[45] P. Hohenberg and W. Kohn, Inhomogeneous electron gas, Phys. Rev. **136**, B864 (1964).
[46] W. Kohn and L. J. Sham, Self-consistent equations including exchange and correlation effects, Phys. Rev. **140**, A1133 (1965).
[47] G. Kresse and J. Furthmüller, Efficient iterative schemes for *ab initio* total-energy calculations using a plane-wave basis set, Phys. Rev. B **54**, 11169 (1996).
[48] G. Kresse and D. Joubert, From ultrasoft pseudopotentials to the projector augmented-wave method, Phys. Rev. B **59**, 1758 (1999).
[49] P. E. Blöchl, Projector augmented-wave method, Phys. Rev. B **50**, 17953 (1994).
[50] J. P. Perdew, K. Burke, and M. Ernzerhof, Generalized gradient approximation made simple, Phys. Rev. Lett. **77**, 3865 (1996).
[51] B. L. Gyorffy, A. J. Pindor, J. Staunton, G. M. Stocks, and H. Winter, A first-principles theory of ferromagnetic phase transitions in metals, J. Phys. F: Met. Phys. **15**, 1337 (1985).
[52] L. Thomas and S. Parkin, Current induced domain-wall motion in magnetic nanowires, *Handbook of Magnetism and Advanced Magnetic Materials* (Wiley, Hoboken, NJ, 2007), pp. 282–302.
[53] D. Hobbs, G. Kresse, and J. Hafner, Fully unconstrained noncollinear magnetism within the projector augmented-wave method, Phys. Rev. B **62**, 11556 (2000).
[54] P. D. Haynes and M. C. Payne, Corrected penalty-functional method for linear-scaling calculations within density-functional theory, Phys. Rev. B **59**, 12173 (1999).
[55] X. Wang, D. sheng Wang, R. Wu, and A. Freeman, Validity of the force theorem for magnetocrystalline anisotropy, J. Magn. Magn. Mater. **159**, 337 (1996).
[56] G. Kresse, M. Marsman, and J. Furthmüller, VASP Manual, http://cms.mpi.univie.ac.at/vasp/vasp/vasp.html.
[57] S. Steiner, S. Khmelevskyi, M. Marsmann, and G. Kresse, Calculation of the magnetic anisotropy with projected-augmented-wave methodology and the case study of disordered $Fe_{1-x}Co_x$ alloys, Phys. Rev. B **93**, 224425 (2016).
[58] The DFT calculations reproduce the symmetry constraints $p_-^{0,z} = p_+^{0,z} = 0$, $p_-^{0,y} = -p_+^{0,y}$, and $p_-^{0,x} = p_+^{0,x}$ within numerical accuracy, which is estimated to be 5×10^{-5} eÅ. It is interesting to note that the components $p_-^{0,x} = p_+^{0,x}$ along the dimer bond, which do not contribute to the DM coupling, are not zero in general. Their values are typically in the range 0.0001–0.005 eÅ,

which is one or two orders of magnitude smaller than the DM-relevant chiral component along $\boldsymbol{r}_{12} \times (\boldsymbol{\mu}_1 \times \boldsymbol{\mu}_2)$.

[59] R. Garibay-Alonso, J. Dorantes-Dávila, and G. M. Pastor, Electronic spin-fluctuation theory of finite-temperature cluster magnetism: Size and environment dependence in fe_N, Phys. Rev. B **79**, 134401 (2009).

[60] The self-consistent calculations of the relative stability between ferromagnetic and antiferromagnetic orders indicate that most dimers with bulk NN distance favor a parallel alignment of the local magnetic moments over an antiparallel alignment. The only exceptions are Sc_2, Cr_2, Mo_2, W_2, and Re_2. In some rare cases, such as Tc_2, the actual ground-state configuration is found to be noncollinear, only slightly more stable than the ferromagnetic order. It is important to note that the magnetic behavior of TMs depends sensitively on the distance between the atoms and their local environment. Therefore, it often changes upon deposition on different substrates or in the case of molecular beams where the interatomic distances are relexed.

[61] G. M. Pastor, J. Dorantes-Dávila, S. Pick, and H. Dreyssé, Magnetic anisotropy of 3*d* transition-metal clusters, Phys. Rev. Lett. **75**, 326 (1995).

[62] G. M. Pastor, J. Dorantes-Dávila, and K. H. Bennemann, Size and structural dependence of the magnetic properties of small 3d-transition-metal clusters, Phys. Rev. B **40**, 7642 (1989).

[63] For several ferromagnetic dimers, such as Fe_2, Mn_2, and Tc_2, we were unable to achieve a sufficiently accurate convergence of the Kohn-Sham equations to reliably compute $\Delta\varepsilon = \varepsilon_+ - \varepsilon_-$ for nearly antiparallel orientation of the local magnetic moments (i.e., $\theta \gtrsim 150^\circ$). This, together with the fact that $\Delta\varepsilon$ vanishes for $\theta \to 180^\circ$, precludes us from reporting $D_{12}^z = \Delta\varepsilon/2\sin(\theta)$ for large θ and explains why some curves in Fig. 6 stop short before reaching $\theta = 180^\circ$.